Appl. Phys. A 86, 415–419 (2007)
DOI: 10.1007/s00339-006-3787-6

Applied Physics A
Materials Science & Processing

Invited paper

S. BANERJEE[1,2]
B. WHITE[1,2]
L. HUANG[1,2]
B.J. REGO[1,2]
S. O'BRIEN[1,2]
I.P. HERMAN[1,2,✉]

Precise positioning of carbon nanotubes by ac dielectrophoresis using floating posts

[1] Nanoscale Science and Engineering Center, Columbia University, New York, NY 10027, USA
[2] Department of Applied Physics and Applied Mathematics, Columbia University, New York, NY 10027, USA

Received: 20 July 2006/Accepted: 3 November 2006
Published online: 19 December 2006 • © Springer-Verlag 2006

ABSTRACT Single-walled carbon nanotubes (SWNTs) have been precisely aligned and positioned in device architectures using ac dielectrophoresis by patterning floating metal posts or strips within the electrode gaps. These structures perturb the electric field, causing local enhancements in the field intensity, as seen in simulation, that guide the nanotubes along a predictable path in given directions, in zigzag patterns, or as single or a sequence of tubes along a series of posts. This method enables the assembly of SWNTs in complex multi-electrode geometries, when specifying the electrode voltages is not sufficient to direct the desired assembly. The device characteristics of the dielectrophoretically-aligned SWNTs are discussed.

PACS 61.46.Fg; 73.63.-b; 87.15.Tt

1 Introduction

As silicon devices approach fundamental scaling limits, there has been intense effort to develop carbon nanotubes for electron transport in the next generation of devices [1]. The small diameter of single-walled carbon nanotubes (SWNTs), along with their long length, low scattering, and almost ballistic transport, makes them very attractive as potential channels in field effect transistors (FETs) [2–4]. Furthermore, efforts have been made to integrate these FETs into logic gates and logic circuits [5]. However, certain fundamental challenges still need to be overcome for nanotubes to be viable as channels and interconnects in FETs.

SWNT devices were first fabricated by dispersing SWNTs in a solvent by ultrasonication and dropping them onto prepatterned electrodes [4]; however, this leads to the random deposition of nanotubes. The polydispersity of tubes and the lack of chirality control imply that semiconducting channels and metallic leads cannot be placed wherever desired, and the precise positioning of nanotubes in devices needs to be addressed. Several methods have been proposed to achieve this, including chemical modification of the substrate [6], growing nanotubes on a substrate directly by chemical vapor deposition [7], the mechanical transfer protocol [8], and the use of dielectrophoresis to position carbon nanotubes in electrode gaps, which leads to much better control of alignment [9–11]. In related work, the contact-free trapping, handling, and trans-

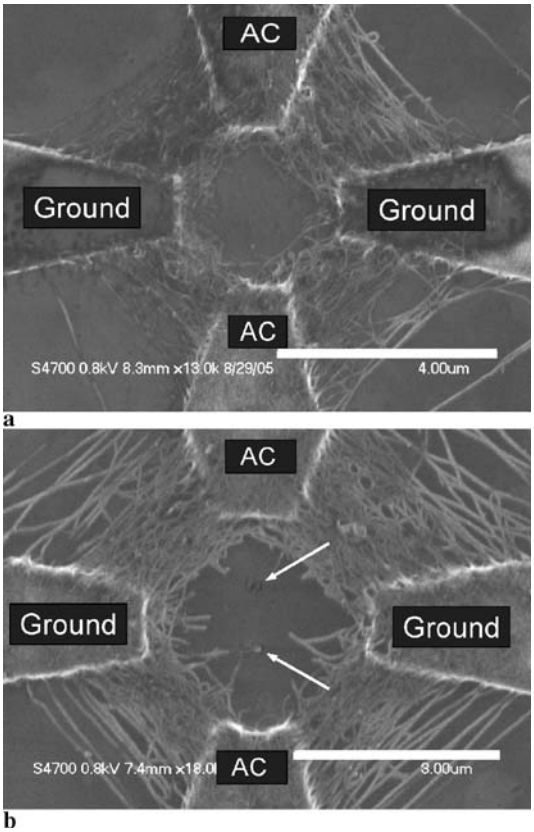

FIGURE 1 (**a**) SEM micrographs showing carbon nanotubes dielectrophoretically aligned along adjacent electrodes by applying the same voltage to an opposing pair of electrodes (8 V, 5 Hz, 3 μm gap), with the other opposing pair grounded. (**b**) Dielectrophoretically aligned tubes as in (**a**) but with two 300 nm diameter posts near the center of the 3 μm gap. All SEM images were obtained on a Hitachi S4700 instrument at an accelerating voltage of 0.8–1.0 kV. The *scale bars* represent 4 μm and 3 μm in (**a**) and (**b**), respectively. *White arrows* are used to point out the two metal posts in the gap, one of which is bright and the other is dark

✉ Fax: +1-212-854-1909, E-mail: iph1@columbia.edu

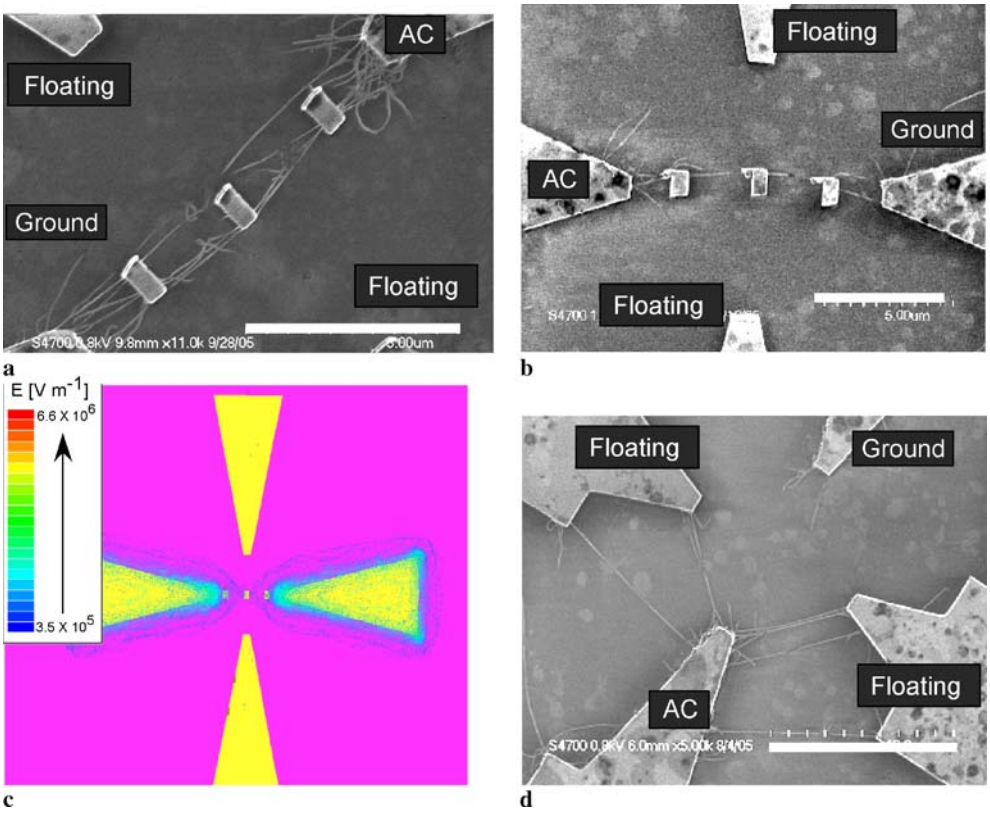

FIGURE 2 (**a**,**b**) SEM micrographs of carbon nanotubes dielectrophoretically aligned in a 10 μm gap using 1 μm wide strips to guide them across. The voltage applied across the opposing electrodes spanning the strips is 8 V peak-to-peak and the frequency is 5 MHz. The other pair of opposing electrodes are floating. 8 μL of NaDDBS wrapped tubes are used. (**a**) Several nanotubes link up segments between the metal strips. (**b**) A single nanotube is guided along the edges of the strips. (**c**) Simulated electric field magnitudes in the presence of gold strips for the exact configuration shown in parts (**a**) and (**b**), with the electric field magnitude increasing from 3.5×10^5–6.6×10^6 V/m linearly from the blue to red color bars. See the caption to Fig. 4 for more information on the simulations. (**d**) Control experiment for the same pattern depicted in (**a**) and (**b**) but without any strips in the gap. All electrodes shown in all figures have tips that are 1 μm wide, except for those in Fig. 3f, which come to a point. *Scale bars* represent 5 μm in (**a**) and (**b**) and 10 μm in (**d**)

fer of small polarizable objects has been demonstrated using open ring electrode structure traps [12, 13]. The availability of micelle wrapped single tubes, which enable aqueous solutions of nanotubes, has permitted much greater control of the ac electric field alignment of individual SWNTs [11, 14], enabling assembly. We report even better controlled placement of SWNTs, in four-electrode geometries, by using floating metal posts to perturb the electric field locally and controllably. This approach can enable the desired placement of SWNTs in multi-electrode structures when controlling the voltages on the electrodes is not sufficient to do so.

The dielectrophoretic force on a particle of dielectric function ε_1 with radius r in a medium of dielectric function ε_2 is

$$\boldsymbol{F}_{\mathrm{DEP}} = 2\pi\varepsilon_1 \mathrm{Re}\left|\underline{K}(\omega)\right| r^3 \nabla E^2_{\mathrm{rms}}\,, \tag{1}$$

where E is the electric field (with rms standing for root-mean-square) and K is the Clausius–Mossotti factor. (The nanotube micelle can be considered to be quasi-spherical.) This factor depends on the difference in the dielectric constants of the particle and the medium (nanotube micelles and water here) [15]

$$\mathrm{Re}\left|\underline{K}\right| = \frac{\varepsilon_2 - \varepsilon_1}{\varepsilon_2 + 2\varepsilon_1} + \frac{3(\varepsilon_1\sigma_2 - \varepsilon_2\sigma_1)}{\tau_{\mathrm{MW}}(\sigma_2+\sigma_1)^2(1+\omega^2\tau^2_{\mathrm{MW}})}\,. \tag{2}$$

The dielectrophoretic force consists of the dielectric and Coulomb forces. The former arises from gradients in the permittivity (first term) and the latter from gradients in the conductivity (σ) (second term). The first term on the right hand side of (2) shows that the higher dielectric function materials are pulled into higher field regions, such as metallic SWNTs in water. For a tube with a cylindrical shape, the dielectrophoresis force is

$$\boldsymbol{F}_{\mathrm{DEP}} = \frac{\pi d^2 l}{8}\varepsilon_l \mathrm{Re}\left(\frac{\varepsilon_t^* - \varepsilon_l^*}{\varepsilon_l^* + (\varepsilon_t^* - \varepsilon_l^*)L}\right)\nabla E^2_{\mathrm{rms}}\,, \tag{3}$$

$$\varepsilon^*_{t,l} = \varepsilon_{t,l} - \mathrm{i}\frac{\sigma_{t,l}}{\omega}\,, \tag{4}$$

where ε_t^* and ε_l^* are the complex dielectric constants of the tube and the surrounding liquid, ε and σ are the corresponding real parts of the dielectric constants and conductivities, L is the depolarization factor, and d and l are the diameter and length of the tube [16].

2 Experimental

HiPCO SWNTs (Carbon Nanotechnologies) were wrapped in a sodium dodecylbenzene sulfonate (NaDDBS) micelle using a modification of the method previously described in the literature, and aqueous solutions of micelle-wrapped SWNTs were used here [17]. Individual tubes or small bundles are expected to be the predominant species dissolved in solution, and have diameters of 0.7–1.1 nm and lengths ranging from ∼ 0.1–15 μm.

SWNTs are aligned between four microfabricated Au electrodes, symmetrically pointing to each other, as in Fig. 1, on top of a 500 nm-thick SiO_2 film atop a Si substrate. The electrode heights range from 200–250 nm and the gaps from 3 μm to 10 μm. In most cases, an ac voltage is applied to opposite electrodes with no load resistor; 8 μL of the nanotube solution is placed in the gap for times varying from 60 s to 4 min. The sample is then washed with the voltage still on using ∼ 800 μL DI H_2O and dried with N_2. Micropatterned

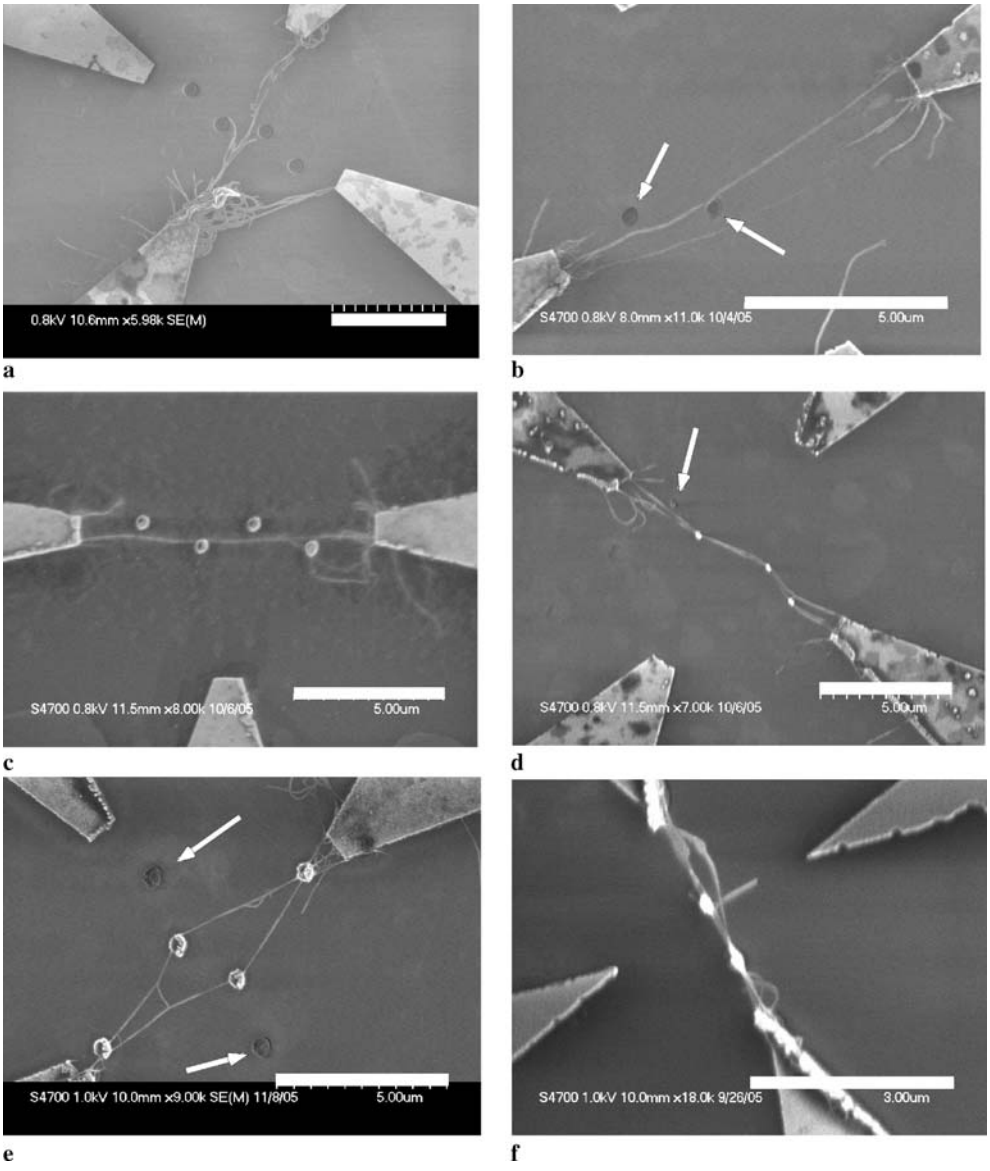

FIGURE 3 Scanning electron microscopy images of dielectrophoretically aligned carbon nanotubes positioned by using metal posts to guide the tubes. (**a**)–(**e**) The applied voltage is 8 V peak-to-peak and the frequency is 5 MHz, across 10 μm gaps. 8 μL of NaDDBS wrapped tubes are used. In (**b**)–(**f**) the electrode pair in line with the posts is powered while in (**a**) the electrode pair normal to the line of posts is powered. (**a**) Tube alignment occurs across the powered pair of electrodes (and to other electrodes as well) when ∼ 600 nm diameter metal posts span the other pair of electrodes. (**b**) Two 500 nm diameter posts guide a single nanotube. (**c**) Tube alignment inline between the 500 nm diameter posts, without necessarily touching all the posts. (**d**) Alignment across posts that are ∼ 300 nm in diameter. (**e**) Alignment across posts that are ∼ 600 nm in diameter. Posts that are closer are preferred over posts that are further away. (**f**) Guided assembly across a 3 μm gap using ∼ 500 nm posts. The electrodes come to a sharp point. The voltage applied is ∼ 6 V and the frequency is 5 MHz. The *scale bars* represent 5 μm in (**a**)–(**e**) and 3 μm in (**f**). *White arrows* are used to point out the dark metal posts in the gap

Au posts (with circular cross section) and strips (with rectangular cross section) are patterned by e-beam lithography in the electrode gap to perturb the electric field (as confirmed by simulations) to help align the nanotubes and guide them across the gaps.

3 Results and discussion

Figure 1 shows four-electrode geometries for which the same 8 V (peak-to-peak), 5 MHz voltage is applied on two opposing electrodes, with the other opposing electrode pair grounded. With the ac voltage applied across adjacent electrodes, the electric field is strong between them and a minimum is created at the center of the gap, and so the SWNTs align sideways between these adjacent electrodes with the central portion completely empty (Fig. 1a). However, in the presence of the two metal posts, several nanotubes point inward as spokes (Fig. 1b). Given the way voltages are applied here, this clearly demonstrates that the locally enhanced fields due to the electrically floating posts markedly affect assembly.

In Fig. 2 the field is applied across two opposing electrodes and the other two electrodes are floating. Without any strips, as shown in Fig. 2d, the tubes tend to be somewhat randomly aligned in the electrode gap with some tubes spanning from the ac powered to the floating side-electrodes. However, in the presence of the patterned metal strips (Fig. 2a and b) or posts (Fig. 3b–f), the SWNTs are guided across from the powered to the opposing grounded electrode without any tubes binding to the other electrodes. The alignment of the nanotubes along the strips is due to local electric field 'hotspots' induced by the metal strips, as shown by the electric field simulation of the configuration in Fig. 2a and b (Fig. 2c and as described below). Most often, a single tube or small bundle is seen bridging the gap, although occasionally multiple tubes bridge portions of the gap to complete the circuit. When the tube is not in electrical contact with the post, the post is dark in the SEM (see white arrows in Fig. 3b,d, and e).

Guiding seems to occur in Fig. 3b and d with the posts between the powered and grounded electrodes (whether or not the posts are bright in the SEM), but not when they span the

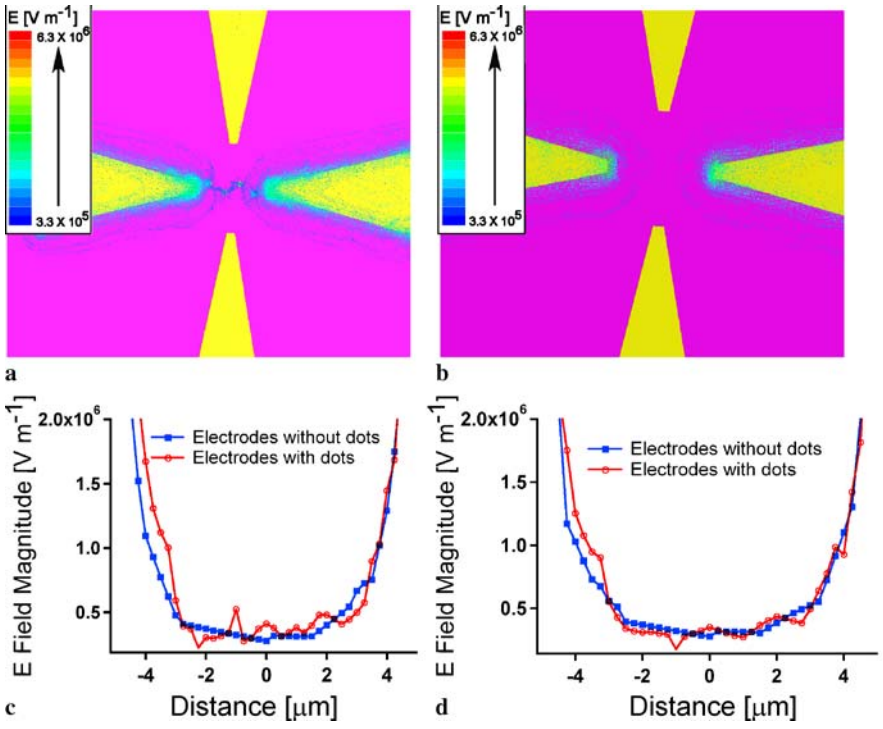

FIGURE 4 The *top panels* show the top views of the calculated electric field magnitude for 10 μm gap electrodes (**a**) with and (**b**) without 500 nm diameter posts. Part (**a**) corresponds to the configuration shown in Fig. 3a and c with four posts. Part (**b**) corresponds to the control experiment shown in Fig. 2d. The SiO_2 surface is shown in pink, while the gold electrodes are shown in yellow. The plotted electric field magnitude increases from a threshold of 3.3×10^5 V/m to 6.3×10^6 V/m, linearly from the blue to red color bars. The highest electric fields, near the electrodes, are denoted by red dots that are too small to be seen here in (**a**) and (**b**). The *lower panels* plot the electric field magnitude across the center of the electrodes for both cases, with (**c**) at the SiO_2 surface and (**d**) 250 nm above the surface

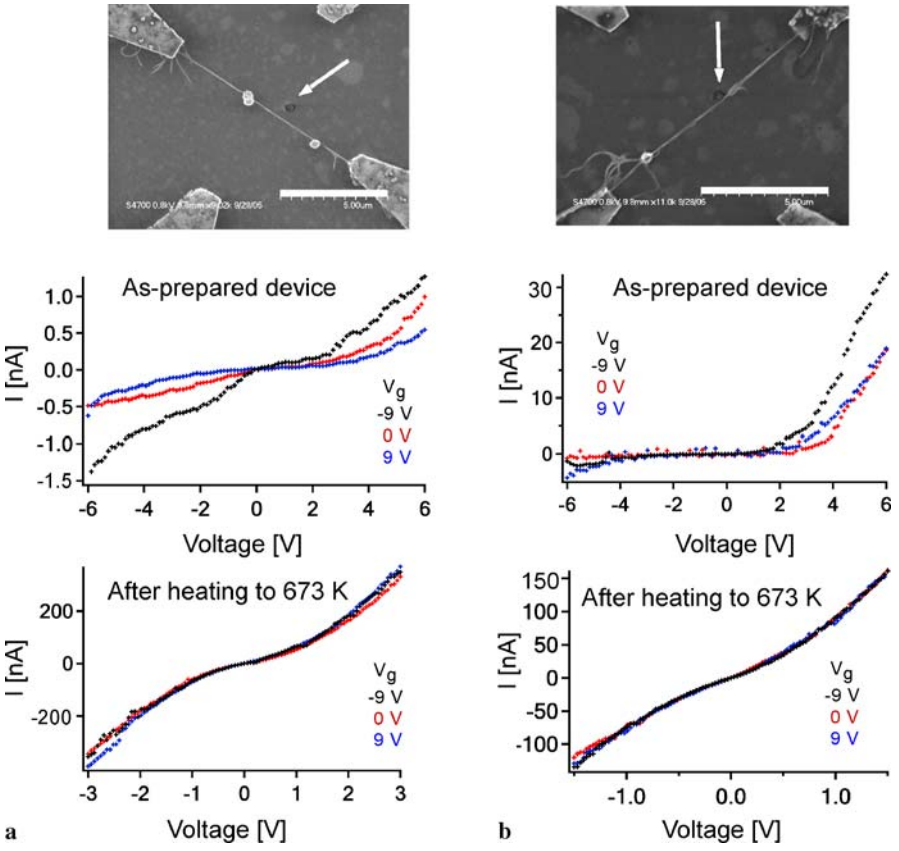

FIGURE 5 SEM images of dielectrophoretically aligned carbon nanotube devices and the *I–V* characteristics before and after heating in N_2 at 400 °C for 10 min. There is considerable dependence of the *I–V* characteristics on gate voltage due to large symmetric barrier heights in (**a**) and rectifying behavior due to asymmetric barrier heights in (**b**). After heating both *I–V* curves become more symmetric. This and the lack of a gate dependence after annealing indicates that these tubes are metallic. The scale bars represent 5 μm in both micrographs

two floating electrodes (Fig. 3a). Two common motifs are observed in this nanotube guiding, a zigzag alignment with the nanotube touching the posts (Fig. 3d) and an inline nanotube alignment between the posts (Fig. 3c). The differences may be related to the ability of an individual nanotube to be bent in the area of the floating potential posts.

To understand the variations in the electric field better in the presence of posts and strips in the gap, the electric fields are simulated using the Maxwell 3D finite element analysis software (Ansoft Corporation, Pittsburgh, PA) for static fields. The Au electrodes and the Si/SiO_2 substrate are included in the simulations. Neumann boundary conditions are assigned

to the outside edges of the problem region and Dirichlet boundary conditions are assigned to the powered electrodes. The simulations in Figs. 2c and 4a and b show that the electric field magnitude is locally enhanced in the vicinity of the posts, so the guiding posts induce local hot spots in electric field magnitude, which likely guide the alignment of the nanotubes across the posts. For example, the zigzag pattern of posts shown in Fig. 3 serves to enhance the electric field in between the post array, leading to the preferential alignment of SWNTs along this array. Figure 4a and b shows the electric field magnitude with and without these posts, for the pattern of Fig. 3c, at the SiO_2 surface (Fig. 4c) and at the height of the top of the electrodes (Fig. 4d). The electric field is enhanced from 3.2×10^5 V/m to almost 5.2×10^5 V/m in some places in between the electrodes at the SiO_2 surface due to the presence of the metal posts.

In Fig. 3a the electrodes spanned by the posts are floating, while the other pair are powered and at ground. Deposition is seen across the powered electrodes and across adjacent electrodes, but not across the electrodes spanned by the posts. This proves that the alignment observed in the other figures is not due to preferred alignment across the higher densities of surfaces provided by the posts (from attractive interactions with the Au surfaces) but to altered electric field patterns. Moreover, Fig. 1b also confirms that this is a field effect and not a chemical one due to bonding to the Au electrode, because the tubes do not touch either post.

Other control experiments indicate that the posts do not trap SWNTs in the absence of a voltage. In fact, upon the application of voltages < 4 V peak-to-peak, no tubes are aligned in the gap, even in the presence of 600 nm diameter posts. From the electric field simulations and experiments using electrodes with and without posts, it seems to be quite clear that the posts align the nanotubes by distorting the electric field and that the assembly of nanotubes does not arise from non-specific sticking interactions with the posts. Notably, micelle-wrapped nanotubes are expected to be much less sticky than pristine nanotubes grown in a CVD environment and used directly.

The I–V curves of the as-prepared SWNTs show a gate dependence and even rectifying behavior, as seen in Fig. 5. The tethering of the tubes at the two electrode ends can differ significantly depending on the surfactant surface coverage, presence of solvent at the contact, and the contact area. In Fig. 5a the I–V curves are only slightly asymmetric, indicating that the Schottky barriers formed at the two electrodes [1] have similar heights. In Fig. 5b, the I–V curves show rectifying behavior, implying that the tunneling barrier at one electrode greatly exceeds the barrier at the other electrode. The large gate dependencies are thought to essentially involve the modulation of the contacts. The (presumably contact) resistance of these device structures are on the order of 1 GΩ.

After heating these structures in N_2 at 400 °C for 10 min, the contact resistance is reduced by about three orders of magnitude and no significant gate dependence is seen any longer; this indicates that these SWNTs are metallic. Such dielectrophoretic selectivity for metallic tubes is most often seen here, as has been predicted by theory [10]. This annealing process clearly lowers the contact barriers very much.

4 Conclusion

In summary, we report a novel method for precisely positioning SWNTs in device architectures by the guiding of metallic posts and strips in four-electrode geometries, where controlling the voltage on the electrodes is not sufficient to direct the desired assembly. The posts provide control of the electric field distribution and do not serve merely as sticking sites. By simulating the electric field in the presence of different arrays of posts and strips, optimized configurations for the predictable positioning of SWNTs can be obtained. This paves the way for using ac dielectrophoresis to align nanostructures in complex circuits. Future work will focus on optimization of the contact resistances and fabrication of more complex hierarchical nanotube device architectures. Such dielectrophoretically positioned metallic tubes could be used for digital sensing and interconnects [18], while semiconducting tubes, which could also be aligned this way, could be used in FET structures for logic operations [1].

ACKNOWLEDGEMENTS The authors thank Shalom Wind for very useful conversations and Ghulam Firdaus for assistance in the early experiments. This work is primarily supported by the Nanoscience Center at Columbia University, which is supported primarily by the Nanoscale Science and Engineering Initiative of the National Science Foundation under NSF Award Number CHE-0 641 523. It is also partially supported from the MRSEC program of the National Science Foundation under Award Number DMR-0 213 574 and by the New York State Office of Science, Technology, and Academic Research (NYSTAR). S.O. also gratefully acknowledges support from the NSF under Award Number ECS-0 507 111.

REFERENCES

1 P. Avouris, Acc. Chem. Res. **35**, 1026 (2002)
2 A. Bachtold, P. Hadley, T. Nakanishi, C. Dekker, Science **294**, 1317 (2001)
3 M.S. Dresselhaus, G. Dresselhaus, P. Avouris (Eds.), *Carbon Nanotubes* (Springer, New York, 2001)
4 S.J. Tans, A.R.M. Verschueren, C. Dekker, Nature **393**, 49 (1998)
5 V. Derycke, R. Martel, J. Appenzeller, P. Avouris, Nano Lett. **1**, 453 (2001)
6 S. Auvray, V. Derycke, M. Goffman, A. Filorama, O. Jost, J.P. Bourgoin, Nano Lett. **5**, 451 (2005)
7 H.J. Dai, Top. Appl. Phys. **80**, 29 (2001)
8 X.M.H. Huang, R. Caldwell, L. Huang, C.J. Seong, M. Huang, M.Y. Sfeir, S.P. O'Brien, J. Hone, Nano Lett. **5**, 1515 (2005)
9 L.A. Nagahara, I. Amlani, J. Lewenstein, R.K. Tsui, Appl. Phys. Lett. **80**, 3826 (2002)
10 R. Krupke, F. Hennrich, H.V. Loehneysen, M.M. Kappes, Science **301**, 344 (2003)
11 H.W. Seo, C.S. Han, D.G. Choi, K.S. Kim, Y.H. Lee, Microelectron. Eng. **81**, 83 (2005)
12 M. Stuke, K. Mueller, T. Mueller, R. Hagedorn, M. Jaeger, G. Fuhr, Appl. Phys. A: Mater. **A81**, 915 (2005)
13 M. Stuke, K. Mueller, T. Mueller, K. Williams, R. Oliver, D.A.A. Ohlberg, G. Fuhr, R.S. Williams, MRS Bull. (2007)
14 Z.B. Zhang, X.J. Liu, E.E.B. Cambell, S.L. Zhang, J. Appl. Phys. **98**, 056 103 (2005)
15 O.D. Velev, In: *Colloids and Colloid Assemblies*, ed. by F. Caruso (Wiley, Weinheim, 2004)
16 R. Krupke, F. Hennrich, M.F. Kappes, H.V. Lohneysen, Nano Lett. **4**, 1395 (2004)
17 M.J. O'Connell, S.M. Bachilo, C.B. Huffman, V.C. Moore, M.S. Strano, E.H. Haroz, K.L. Rialon, P.J. Boul, W.H. Noon, C. Kittrell, J.P. Ma, R.H. Hauge, R.B. Weisman, R.E. Smalley, Science **297**, 593 (2002)
18 J.D. Beck, S. Lu, M.S. Marcus, R.J. Hamers, Nano Lett. **5**, 777 (2005)